

# Sliding Mode Load Observer for a PMSM system

Barna Temesi

**Abstract**—This short design documentation presents the used system model, parameters and load observer. The used observer is a first-order sliding mode observer. The estimated signal is then used for feedforward compensation.

*Index Terms:* dynamic modelling of synchronous motors,  $dq$ -reference frame, PMSM, Load torque estimation, Sliding Mode Observer

## 1 INTRODUCTION

As in every design process, after the problem statement, the system has to be modeled and analyzed. This starts with an overview of the motor parameters. Next, the motor voltage equations, which are already given in the  $dq$ -reference frame, are examined. The mechanical equation of the motor is also presented.

This documentation does not consider the FOC used in the system. The focus is strictly on the rotor position estimator.

The load torque estimator is heavily based on / inspired by the estimator proposed in [5].

Table 1: System parameters, from previous projects such as

Description	Notation	Value	Unit
Number of pole pairs	$N_{pp}$	4	-
Winding resistance	$R_w$	0.19	$\Omega$
Total system resistance	$R_s$	0.268	$\Omega$
q and d-axis inductance	$L_m$	2.2	mH
Rotor PM flux linkage	$\lambda_{mpm}$	0.12258	Wb
Rated speed, SPMSM	$\omega_{m, rated}$	4500	rpm
Rated torque, SPMSM	$\tau_{m, rated}$	20	Nm
Rated power, SPMSM	$P_{m, rated}$	9.4	kW
Rated speed, IM	$\omega_{IM, rated}$	1400	rpm
Rated torque, IM	$\tau_{IM, rated}$	14	Nm
Rated power, IM	$P_{IM, rated}$	2.2	kW
Rated current, VSI	$I_{VSI}$	35	A
IM machine inertia	$J_{IM}$	0.0069	$kg \cdot m^2$
SPMSM machine inertia	$J_{SPMSM}$	0.0048	$kg \cdot m^2$
Total system inertia	$J_{sys}$	0.0146	$kg \cdot m^2$
Coulomb friction	$C$	0.2295	Nm
Viscous friction	$B$	0.0016655	N

## 2 MODEL OF THE SYSTEM

The motor, in the scope of this thesis, is an SPMSM. This means that the permanent magnets are located on the surface of the rotor. Due to this, the motor is non-salient, and also the reluctance path is equal on the d- and q-axis. This results in equal inductance on the d- and q-axis. For easier understanding, the machine inductance will be denoted as  $L_s$  [2].

$$L_d = L_q = L_s \quad (1)$$

The most important parameters of the motor and the other necessary system parameters are listed in the table 1.

As can be seen from the table, the motor has 4 pole pairs. Generally speaking, this means that the machine is more geared towards high-speed operation. In high-torque operation applications, like in the case of a steering motor, the number of poles might exceed a 100.

In simulations, the total system resistance will be used, which takes into account the resistance of every possible component in the setup [1].

The motor voltage equations are shown in equation (2). Due to the assumption that the system is symmetrical and balanced, the zero term ( $v_0$ ) is zero.

$$\begin{aligned} v_d &= R_s i_d + p \lambda_d - \omega_r \lambda_q \\ v_q &= R_s i_q + p \lambda_q + \omega_r \lambda_d \\ v_0 &= 0 \end{aligned} \quad (2)$$

In the  $abc$ -reference frame, the machine flux-linkage is dependent on position and the machine inductance is constant for a non-salient pole machine, but because the model is already transformed into the  $dq0$ -reference frame, the machine inductance is constant.

The stator  $dq0$ -reference frame is aligned with the rotor reference frame, which is naturally in the  $dq0$ -reference frame. The rotor  $d$ -axis is chosen to be aligned with the maximum flux density line at no load condition. The  $q$ -axis is always leading the  $d$ -axis by 90 degrees electric. This way, it is aligned with the minimum flux density line [1].

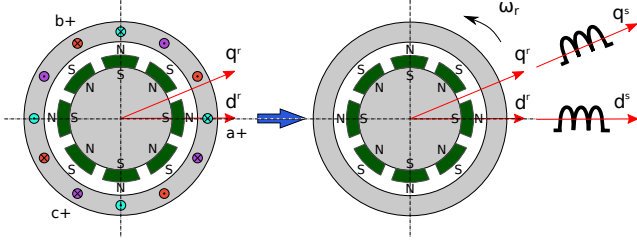


Figure 1: Reference frame transformation from *abc* to *dq*. The structure of the motor is also shown. Inspiration: [3]

The two *d*-axis is in line now. This is convenient because, it results in the *d*-axis and the *q*-axis flux-linkage as shown in equation (3).

$$\begin{aligned}\lambda_d &= (L_{ls} + L_{md}) i_d + \lambda_{mpm} = L_d i_d + \lambda_{mpm} \\ \lambda_q &= (L_{ls} + L_{mq}) i_q = L_q i_q \\ \lambda_0 &= 0\end{aligned}\quad (3)$$

After substitution, the voltage equations may be rewritten as seen in equation (4).

$$\begin{aligned}v_d &= R_s i_d + p(L_d i_d + \lambda_{mpm}) - \omega_r L_q i_q \\ v_q &= R_s i_q + p(L_q i_q) + \omega_r (L_d i_d + \lambda_{mpm})\end{aligned}\quad (4)$$

Where  $p$  is the differential operator  $\frac{d}{dt}$ . Differentiating the equation, keeping in mind that the derivative of a constant is zero, will result in the following.

$$\begin{aligned}v_d &= R_s i_d + L_d p i_d - \omega_r L_q i_q \\ v_q &= R_s i_q + L_q p i_q + \omega_r (L_d i_d + \lambda_{mpm})\end{aligned}\quad (5)$$

In one more step, the homogeneous first-order differential equation of the system is acquired.

$$\begin{aligned}\frac{d}{dt} i_d &= -\frac{R_s}{L_d} i_d + \frac{1}{L_d} v_d + \omega_r \frac{L_q}{L_d} i_q \\ \frac{d}{dt} i_q &= -\frac{R_s}{L_q} i_q + \frac{1}{L_q} v_q - \omega_r \frac{L_d}{L_q} i_d - \frac{1}{L_q} \omega_r \lambda_{mpm}\end{aligned}\quad (6)$$

Equations (4) also contain the back-EMF voltage components which are very important in position estimation, hence they are highlighted here:

$$\begin{aligned}e_d &= -\omega_r L_q i_q \\ e_q &= \omega_r (L_d i_d + \lambda_{mpm})\end{aligned}\quad (7)$$

The governing torque equation can be derived from the equation of the input power of the windings. Simplifying this equation, using the attributions of the SPMSM machine, yields the following expression:

$$T_e = \frac{3}{2} N_{pp} (\lambda_d i_q - \lambda_q i_d) \quad (8)$$

$$T_e = \frac{3}{2} \frac{N_{poles}}{2} (\lambda_{mpm} i_q + (L_d - L_q) i_d i_q) \quad (9)$$

$$T_e = \frac{3}{2} N_{pp} (\lambda_{mpm} i_q) \quad (10)$$

Using Newton's second law, the mechanical equation of the system can be derived as shown in equation (11) [1].

$$T_e = J \frac{d\omega_m}{dt} + B_m \omega_m + T_{dist} \quad (11)$$

Where  $J$  is the total system inertia and  $T_{dist}$ , the disturbance torque, consists of the load torque and Coulomb friction. The total system inertia includes the inertia of both the IM and PMSM machine and also the coupling and fastening components between them.

The first term is related to the torque needed to accelerate the system without friction, the last two terms are related to the torque which is needed to overcome the viscous friction and the disturbance torque, respectively.

### 3 LOAD TORQUE IDENTIFICATION (LTID)

As it was stated in the introduction section, this estimator is heavily inspired by the following publication: [5]. The steps of the design of the observer are presented in this section.

Start by deriving the mechanical equation of the system using Newton's  $2_{nd}$  law. This is shown in (12).

$$j_{red} \dot{\omega}_m = \sum T_{sum} \quad (12)$$

Detail this, such as:

$$j_{red} \dot{\omega}_m = T_m - T_{load} - B_{m,red} \omega_m - T_{dist,residual} \quad (13)$$

Where, the actuator dynamics are shown in (14). The actuator dynamics were reduced to first-order.

$$\dot{T}_m = \frac{1}{\tau_m} (T_{m,ref} - T_m) \quad (14)$$

Transforming the system to the standard form yields the next:

$$\dot{\mathbf{x}} = \mathbf{f} + \mathbf{b}u \quad (15)$$

$$\begin{aligned}f &= \frac{1}{j_{red}} (-T_{load} - B_{m,red} \omega_m - T_{dist,residual}) \\ b &= \frac{1}{j_{red}} \\ u &= T_m\end{aligned}\quad (16)$$

### 3.1 Sliding Mode Load Observer (SMO)

Define the surface in the following equation (17).

$$\sigma = \hat{\omega}_m - \omega_m = \tilde{\omega}_m \quad (17)$$

The observer law was proposed in [5], such as:

$$\dot{\omega}_m = \frac{1}{J_{red}}(T_m - B_{m,red}\omega_m) - Z_s \quad (18)$$

Furthermore,  $Z_s$  equals:

$$Z_s \approx \hat{T}_{load} + \hat{T}_{dist,residual} \quad (19)$$

Where,  $\hat{T}_{dist,residual}$  stands for all of the un-modelled terms. In this case, the most important neglected terms are the following: static friction ( $T_{fric,static}$ ) and non-linear friction ( $T_{fric,nonlin}$ ). It is worth noting here that these effects could be captured by usage of the LuGre friction model (first publication by: Karl Johan Åström). However, this would increase the number of parameters by six. Thus, the system complexity, system identification and / or tuning effort would be greatly increased.

The sliding term  $Z_s$  is shown in (20). It was made discontinuous across the sliding surface to account for uncertainties, un-modelled high-frequency dynamics, unknown disturbances.

$$Z_s = \rho_{obs} \text{sgn}(\sigma) = \rho_{obs} \text{sgn}(\tilde{\omega}_m) \quad (20)$$

Where,  $\rho_{obs} > 0$  and the lower bound of it is calculated using Lyapunov theory. The proof of stability using Lyapunov theory is not presented in this document.

The output of the observer is:  $\hat{T}_{load}$ , it is filtered by a first-order LPF.

$$\hat{T}_{load} = -Z_s \frac{\omega_c}{s + \omega_c} \quad (21)$$

To further smooth the output signal, the *sign* function can be substituted. The options are the next:

The sigmoid function, defined in equation (22)

$$F = \frac{\sigma}{\text{abs}(\sigma) + \epsilon} \quad (22)$$

Or the saturation functions, which is shown in (23).

$$\text{sat}(\sigma/\phi) = \begin{cases} \sigma/\phi & |\sigma/\phi| \leq 1 \\ \text{sgn}(\sigma/\phi) & \text{otherwise} \end{cases} \quad (23)$$

### 3.2 Observer Structure

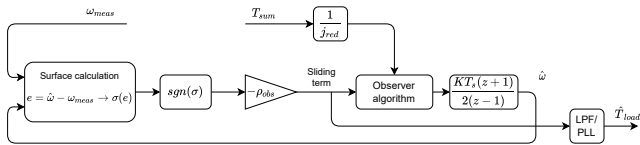


Figure 2: Structure of the Sliding Mode Load Observer

## 4 CONCLUSION

For further information, proof of stability, simulation results, experimental data, please see [5].

## REFERENCES

- [1] B. Temesi, U. G. Gautadottir, *Sensorless Control of PMSM Drive Using Sliding-Mode-Observers* AAU, Denmark, 2020 Master's thesis.
- [2] D. Wilson, *Motor Control Compendium*, 1st-ed . 2011
- [3] K. Lu, *Control of Electrical Drive Systems and Converts Lecture 1 Slides*, 1st-ed . pp. 1-30, 2019
- [4] J. E. Slotine, W. Li *Applied Nonlinear Control* Englewood Cliffs, New Jersey: Prentice Hall, 1991.
- [5] W. Lu, Z. Zhang, D. Wang, K. Lu, D. Wu, K. Li, L. Guo, *A New Load Torque Identification Sliding Mode Observer for Permanent Magnet Synchronous Machine Drive System* in IEEE Transactions on Power Electronics, vol. 34, no. 8, pp. 7852-7862, Aug. 2019, DOI: 10.1109/TPEL.2018.2881217.